

Morphology of Ionic Micelles as Studied by Numerical Solution of the Poisson Equation

Olga S. Zueva, Vladimir S. Rukhlov, and Yuriy F. Zuev*

Cite This: *ACS Omega* 2022, 7, 6174–6183

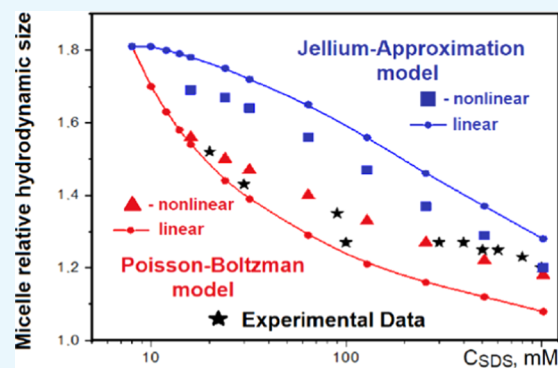
Read Online

ACCESS |

Metrics & More

Article Recommendations

ABSTRACT: The existing concepts of the ionic micelle structure were specified. It was noted that the composition of dispersed phase particles in a liquid dispersion medium should necessarily include adsorbed counterions rigidly bound to these particles. By numerical solution of the Poisson equation for the two most often used approximations, the Poisson–Boltzmann (PB) model and the Jellium-approximation (JA), the electric potential decay from the Stern potential of dispersed phase particles was defined. A new methodological approach to analyze the reaction of micelle potential decay based on small variability of the CMC value was proposed. It made possible to determine the dimension parameter, which in the presence of weak thermal effects approximately corresponds to the micelle hydrodynamic radius, and to calculate the electrokinetic potential of micelles. The results of theoretical calculations were compared with our previous experimental data on the thickness of the SDS micelle hydrophilic layer obtained by SAXS. A good agreement between the calculated and measured values was obtained, and it was noted that for low concentrations the experimental values are more correctly described by the PB model, but for concentrations greater than 100 mM the JA model is more preferable. It was found that the slipping plane is located near the outer Stern plane and is separated from it only by a few molecular layers of water. The influence stronger than the thermal one can shift the slipping plane closer to the micelle core. Accordingly, the smallest hydrodynamic micelle size is determined by the outer Stern plane. The results of our work allowed us to conclude that the micelle is not something soft and watery, but according to its specified structure, it is a more solid-like particle than was previously assumed. The proposed approach can be extended to investigate other effects of a physicochemical nature, in particular, those observed with the addition of an external electrolyte or nanoparticles.



INTRODUCTION

Surfactants in molecular form and organized assemblies are of great fundamental, technological, and commercial interest stimulating further insight into their physical–chemical properties and enormous prospective applications, including pharmacology, agrochemistry, household chemistry, cosmetics, biotechnology, and nanomedicine.^{1–5} In addition, surfactants are of considerable importance in the oil industry, for example for enhanced oil recovery, oil transportation and processing.^{6–9} Many novel technologies are difficult without nanoparticle stabilization in water or oil. In particular, surfactants are needed for obtaining carbon nanotube dispersions.^{10–13} The development of surfactant-based technologies and applications demands reliable information about the physicochemical characteristics of surfactants in various structural states.

The present study is performed in view of the critical analysis of the existing picture on micelle morphology and size in water solution of ionic surfactants. The motivation of this work is based on the variety of structural definitions^{14,15} and the contradictory experimental data on micelle structure (morphology) known from the literature.^{16–32} Unfortunately,

the published measured and calculated values for the micelle basic sizes, for example for the most representative ionic surfactant sodium dodecyl sulfate (SDS), differ among themselves significantly. So, for the radius of the SDS micelle hydrocarbon core, the values vary from 1.50 to 1.93 nm.^{16–24} The size of the micelle central part (named aggregate of surfactant ions, micellar particles, solid phase particles) was estimated as 2–2.5 nm,^{25–31} and its hydrodynamic radii were evaluated as 3–3.2 nm (at 10 mM)²⁹ and as 3.5 nm (at 20 mM).³² With all this going on, the micelle size determination has been often undertaken at various concentrations and using different methods that are sensitive to different physical peculiarities of micelles. Also, the discrepancies in micelle size

Received: November 24, 2021

Accepted: February 1, 2022

Published: February 10, 2022



In addition, the modified models of micelle morphology are known, for instance, the Stern–Graham model,⁴⁴ associated with the separation of the adsorption layer into two parts: (1) the Helmholtz ionic monolayer with rigidly adsorbed dehydrated counterions is the closest to the micelle core and (2) the successive layer with hydrated counterions occupying several interatomic distances. In this case, the layer with hydrated counterions is called the Stern layer, and its boundaries are called the inner and outer Stern planes. The thickness of the Stern layer (outer Stern plane) is determined by the size of the solvent-separated ion pair (linking the surfactant ion and the counterion).^{34,45} The shell of the micelle hydrocarbon core, including the Helmholtz–Stern layer, represents the concentrated mixture of hydrocarbons, electrolyte, and water having unique structural and chemical properties, which promotes various chemical processes.^{46–48} Immediately after the Helmholtz–Stern layer the diffuse part of the ionic double layer is located containing all of the remaining counterions. This ionic atmosphere of the micellar particle is formed due to the thermal motion of counterions in an attractive electrostatic field of a charged micelle surface, which tends to equalize counterion concentration within the solution bulk.^{39,49} The first few water layers, located immediately after the Helmholtz layer, are bound rather rigidly to the micelle core having increased local viscosity. Because of the hindered orientation mobility of bound water molecules its local permittivity is sufficiently small.⁵⁰

Under the influence of some physical forces (e.g., electric, magnetic, acoustic in nature) or under the ordinary thermal Brownian motion the micelle double ionic layer gets disturbed. The interface, which separates bound and bulk water, is called the slipping (shear) plane. Its radius determines another micellar characteristic dimension, called the micelle hydrodynamic radius r_{ζ} , which is often considered the micelle size (Figure 1). The electric potential at the slipping plane is called the electrokinetic or ζ -potential.

The location of the slipping plane depends on magnitude of the applied external disturbance. Therefore, the micelle slipping plane can slightly alter its position in different experiments even at equal surfactant concentrations and temperatures, or we can assume that micelles have a slipping layer of a certain thickness instead of the slipping plane. This slipping layer should be located outside the Helmholtz–Stern layer right after the layer of bound water with high ordering and increased viscosity. It may be suggested that in the presence of strong intermicelle interactions in concentrated systems, the slipping planes may drift closely to the outer Stern surface. The weaker action will hold the slipping plane away from the micelle center. The lower limit of ζ -potential corresponds to the weakest influence on the position of the slipping plane, corresponding only by the Brownian thermal motion. The hydrodynamic radius of micelles r_{ζ} has the maximum value in the presence of only thermal impact. In the absence of external disturbances, the ambiguity in determining the hydrodynamic radius and ζ -potential of micelles disappears.

The value of ζ -potential is determined by electric charges bounded by the slipping plane and therefore indicates the degree of electrostatic repulsion of micelles. It is known⁵¹ that a ζ -potential greater than 30 mV (positive or negative) indicates the stability of colloid dispersions. Any additional influence (for example, by ultrasound) leads to the displacement of the slipping plane closer to the micelle core, resulting

in a decrease of the hydrodynamic radius r_{ζ} , an increase of the ζ -potential, and in the advancement of dispersion stability as a whole.

Problem Formulation. A spherical micelle, as a structural arrangement is characterized by sizes and potentials associated with them: radius of the micellar particle $R_{\text{mic}} = a$ (for simplicity, in the following we will use designation a for the radius of a micellar particle or micelle core) and its surface potential $\Psi(R_{\text{mic}}) = \Psi(a)$, as well as the hydrodynamic radius of micelle r_{ζ} and its electrokinetic or ζ -potential.^{39,40} Since there is no theoretical relation between these parameters, we have tried to eliminate, in the present work, the existing inconsistencies. In our calculation model, we are proceeding from the fact that the slipping (shear) surface divides the solution around a micelle into two parts, differing in viscosity. The potential decay curves calculated by us numerically indicate the existence of two regions associated with an uneven decrease in the bulk density of counterions with an increase in distance from the micellar particle when very fast potential decay turns into a very slow one. So, the enlarged counterion concentration near micelle can be associated with the increased solution viscosity, and the breakpoint of decay can be correlated with the hydrodynamic radius of micelles. However, it is impossible to specify this distance only by the shape of numerically calculated decays. Therefore, we have developed a new approach that allowed us to determine this boundary distance.

The novelty of our study is the proposed methodological approach to analyze the reaction of micelle potential decay on small variability of the CMC value. Since different experimental techniques demonstrate the abrupt change in various physical–chemical properties of surfactant solution upon micellization³⁷ in some concentration range near the average CMC value, we assumed that the proposed approach would take into account small fluctuations of the micelle microenvironment, inevitable upon micellar transition. As a result, we determined that at certain distances from the micelle core there is the region with redistribution of counterion density (concentration) with a well-marked maximum. We tried to relate the determined position of this maximum r_{max} to the micelle hydrodynamic radius r_{ζ} as well as to the Debye length. The validity of the developed approach was successfully confirmed by the obtained agreement between calculated positions of maxima and our early experimental SAXS results on the thickness of the hydrophilic layer of SDS micelles.³²

In the theoretical computations of parameters for the diffuse part of the micelle double ionic layer the finite size of ions is ignored. The self-consistent field method is used in our calculations. The independent motion of ions in this field is allowed. In the framework of the applied method the electrostatic potential $\Psi(r)$, created near the spherical micellar core, and the electric field strength $E(r) = -d\Psi(r)/dr$ at the point with radius vector r from the center of the micelle are associated with the spatial distribution of charge density around the micelle by means of the Poisson equation⁴⁰

$$\frac{1}{r^2} \frac{d}{dr} \left(r^2 \frac{d\Psi}{dr} \right) = \rho / (\varepsilon \cdot \varepsilon_0) \quad (1)$$

where ρ is an average charge density at the point of the diffuse layer, where potential is calculated, ε is the dielectric permittivity of the continuous phase (water), and ε_0 is the electric constant (SI system is used). The Poisson equation is supplemented with the boundary conditions, according to

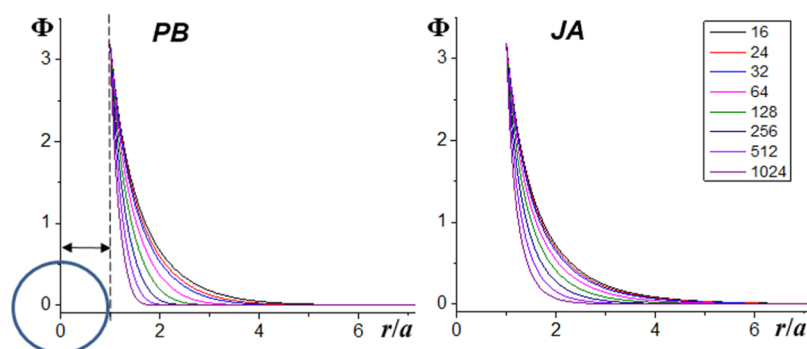


Figure 2. Decays of dimensionless potential of SDS micelles calculated within the PB (left) and JA (right) models for nonlinear approximation as a function of r/a for eight surfactant concentrations indicated in order, increasing from right to left.

which the potential changes from the value $\Psi(a)$ on the surface of the micelle core to zero at infinity. The main problem in solving eq 1 is the determination of the spatial charge density distribution ρ and its dependence on potential Ψ .

The results can be generalized over the case of a 1–1 electrolyte using the approach described in the paper.⁵² When solving the Poisson equation, one usually operates with the dimensionless potential $\Phi = \pm e \cdot \Psi(r)/(k \cdot T) = \Psi(r)/\Psi_0$, where e is the elementary charge and k is the Boltzmann constant. For temperature $T = 298$ K, the combination of constants is equal $(k \cdot T)/e = \Psi_0 = 25.7$ mV. The choice of the sign on the right-hand side of this relation is defined by the condition that the dimensionless potential Φ must be essentially positive. Since the surface potential of micellar core $\Psi(a)$ is usually equal to dozens of millivolts the value of the dimensionless potential $\Phi(a) = \Phi_0$ corresponds to several units. It means that the ratio $\Phi_0 \ll 1$ used for certain approximations⁴⁰ does not satisfy the case of surfactant micelles. In particular, in the case of sodium dodecyl sulfate (SDS) the known values on the micellar core surface potential are very inconsistent (ranging from -60 to -140 mV).^{20,27,30,53} It is known that for $\Psi(a) = -82$ mV the calculations give $\Phi_0 = 3.19$.⁵³

There are various approaches to simplify the Poisson equation, associated with the description of ion distribution in solution using various models.^{54–57} Usually to describe the disordered concentrated solutions, the concept of ionic strength I is introduced

$$I = \frac{1}{2} \sum C_i Z_i^2 \quad (2)$$

which highlights not only the ions concentration in solution but also the magnitude of the ion–ion electrostatic (Coulomb) interactions. Here, C_i is the concentration of the type i ions in solution and Z_i is their charge number. In the pre-micellar state, the ionic strength is equal to the surfactant concentration, i.e., $I = C$. For the case of the micellar solution, the concept of ionic strength becomes ambiguous, depending on the choice of the model describing charge distribution in solution. Two of the most often used models are the Poisson–Boltzmann (PB) and the Jellium-Approximation (JA) ones. The PB model assumes that a spatial distribution of all particles, including micelles, is described by the Boltzmann distribution. In the PB model, micelles are identified with multiple charged ions with a strong Coulomb repulsion.⁵⁸ Such a picture of micelle solutions leads to the interrelation

$$I = C_{\text{CMC}} + (\alpha/2)(C - C_{\text{CMC}})(1 + \alpha N_{\text{agg}}) \quad (3)$$

In the JA model, it is assumed that the uniformly distributed micelles, located in solution near the equilibrium positions, are surrounded by the ionic atmosphere, which obeys the Boltzmann distribution. For these models, the simplified form of the Poisson equation (but still requiring numerical solution) is given below in the next section. In the JA model, micelles are the isolated objects with zero total charge due to the ordered arrangement of counterions around micelles.^{20,59} In this case, the ionic strength of surfactant micellar solution I is determined according to another relation

$$I = C_{\text{CMC}} + (\alpha/2)(C - C_{\text{CMC}}) \quad (4)$$

The distribution of micelles over the bulk is determined not by their Coulomb repulsion but according to the statistical nature of solution disorganization, which is responsible for the thermal motion of particles. In the paper,⁶⁰ four methods of the ionic strength calculation were considered. It was noted that SDS micelles make significant contributions to solution conductivity but not to the effective ionic strength. Also, it was shown that for the ionic strength calculation it is more correct to use relation (4).

Dimensionless Micelle Potential in Linear Approximation. It is known that for the case of a small electrostatic potential of particle surface, i.e., for $\Phi_0 \ll 1$, the Poisson equation for both models in linear approximation reduces to the form⁴⁰

$$\frac{1}{r^2} \frac{d}{dr} \left(r^2 \frac{d\Phi}{dr} \right) = (2e^2 I / \epsilon \cdot \epsilon_0 k T) \Phi = (1/\lambda)^2 \Phi \quad (5)$$

This equation can be solved not only numerically but also analytically. For this case the Debye length $\lambda = (\epsilon \cdot \epsilon_0 k T / 2e^2 I)^{1/2}$, determined by the ionic strength I , is introduced to describe the properties of the system. The numerical value of parameter λ depends on the concentration of ions in solution, namely, on the ionic strength of solution. In the case of flat charged surface, the parameter λ has a simple physical meaning specifying the distance at which the potential decreases $e = 2.72$ times. Despite the fact that for spherical particles this interpretation ceases to be valid, the Debye length λ , which is related to the potential decay rate is compared with the thickness of the ionic atmosphere around a charged spherical particle. This approach is not very correct for micelles since the approximation $\Phi_0 \ll 1$ is not satisfied here. However, the simplicity of calculating the parameter λ and the possibility to write down the analytical expression for potential decay allow

us to use eq 5 to compare the obtained micelle parameters for two models. A comparison of Debye lengths performed for two models in linear approximation showed that $\lambda_{PB} < \lambda_{JA}$, since at equal surfactant concentrations the ionic strength value in the PB model is much larger compared with the JA one. This means that in the PB model potential decreases faster and the thickness of ionic atmosphere around micelle is less than that for the JA model. The solution of eq 5 for $r > a$ represents the following function⁶¹

$$\begin{aligned}\Phi &= \Phi_0 \frac{a}{r} \exp[-(r-a)/\lambda] \\ &= [\Phi_0/(r/a)] \exp[-(r/a-1)/(\lambda/a)]\end{aligned}\quad (6)$$

For linear approximation the shape of potential decay $\Phi(r/a)$ as the function of relative distance for $r > a$ has a shape similar to the curves shown in Figure 2 (obtained for nonlinear approximation). They are characterized by a very sharp decrease in the range of r values close to a and by a much slower decay at a large distance. The range, where noticeable changes in potential are detected, is several (3–4) times greater than λ . Therefore, in many studies, the parameter λ is compared not with the actual thickness of the ionic atmosphere but with a distance to the micellar slipping plane. However, this approach also has certain drawbacks. In particular, the calculations show that at this distance the numerical values of Φ are too small to correspond to ζ -potential because of the exponential potential decay. For real micelles, when the condition $\Phi \ll 1$ is not satisfied, the shape of potential decay is changed, the introduction of the constant λ becomes incorrect, and relation (5) for calculation of the ionic atmosphere thickness λ can no longer be applied. Thus, for the case of highly charged particles the equations exist, which allows numerical calculation of the dimensionless potential decay at various surfactant concentrations. However, there is no criterion, which allows correct estimation of the ionic atmosphere thickness and its alteration in the presence of impacts of any physical or chemical nature.

Dimensionless Micelle Potential in Nonlinear Approximation. For numerical calculations within the PB and JA models the transformed Poisson equation⁵⁷ was used. For the case of the 1–1 valence ionic surfactant in the presence of the external 1–1 electrolyte with concentration C_E the equations for both PB and JA models can be written in the common form

$$\begin{aligned}\frac{1}{r^2} \frac{d}{dr} \left(r^2 \frac{d\Phi}{dr} \right) &= (\epsilon^2/\epsilon \cdot \epsilon_0 kT) [2(C_{CMC} + C_E) \sinh(\Phi) \\ &+ \alpha(C - C_{CMC})(\exp \Phi - 1 + A_{PB})]\end{aligned}\quad (7)$$

In the PB model, there is an additional term $A_{PB} = 1 - \exp[-Z\Phi]$, where $Z = \alpha N_{agg}$ is the charge number of the micelle core. In the JA model, this term is absent. For both models, the equations require a numerical solution.

It should be noted that all calculations were carried out within the selected models, which require the experimentally defined data on the size of micelle core a , the potential of its surface $\Psi(a)$, the number of surfactant aggregation in micelle N_{agg} , the degree of micelle ionization α , and the critical micelle concentration C_{CMC} . The following parameters for SDS micelles were used in our calculations: $N_{agg} = 64$, $a = 2.3$ nm, $C_{CMC} = 8$ mM, and $\Psi(a) = -82$ mV. We have taken the value $\alpha = 0.25$, although the known values at $T = 298$ K lie in

the interval 0.25–0.29.^{41,60,62,63} The choice of SDS was specified by its prevalence in scientific studies and our experience to work with SDS.^{12,13,32,33}

To numerically solve the resulting equations the `bvpsuite1.1` software package was used.⁶⁴ The results of calculations coincide with the results of the paper⁶⁵ and with those in the paper.⁶⁶ This software package was used to calculate the dependence of dimensionless micellar potential on the relative distance from the micelle core surface and to compare the obtained results for nonlinear approximation within the PB and the JA models. For both models in the absence of an external electrolyte (hereinafter $C_E = 0$), the decrease in dimensionless potential of SDS micelle was calculated for eight surfactant concentrations (16, 24, 32, 64, 128, 256, 512, and 1024 mM) at $T = 298$ K as a function of relative distance r/a . The obtained results, shown in Figure 2, Tables 1 and 2 depict the main parameters for both PB and JA models, calculated in the framework of both linear and nonlinear approximations.

Table 1. Ionic Strength I , Relative Debye Length Λ , and Value r_{max}/a at Different Surfactant Concentrations C for the PB Model^a

C (mM)	D (nm)	D/2a	I_{PB}	linear approximation		nonlinear approximation	
				Λ_{PB}	r_{max}/a	r_{max}/a	Λ_{PB}
16	23.7	5.15	25	1.83	1.54	1.56	1.85
24	18.8	4.09	42	1.64	1.44	1.50	1.75
32	16.4	3.57	59	1.54	1.39	1.47	1.69
64	12.4	2.69	127	1.37	1.29	1.40	1.56
128	9.61	2.09	263	1.26	1.21	1.33	1.44
256	7.55	1.64	535	1.18	1.16	1.27	1.34
512	5.96	1.30	1079	1.13	1.12	1.22	1.27
1024	4.72	1.03	2167	1.09	1.08	1.18	1.21

^aD and D/2a are explained in the text.

Table 2. Ionic Strength I , Relative Debye Length Λ , and Value r_{max}/a at Different Surfactant Concentrations C for the JA Model^a

C (mM)	D (nm)	D/2a	I_{JA}	linear approximation		nonlinear approximation	
				Λ_{JA}	r_{max}/a	r_{max}/a	Λ_{JA}
16	23.7	5.15	9	2.39	1.78	1.69	2.17
24	18.8	4.09	10	2.32	1.75	1.67	2.12
32	16.4	3.57	11	2.26	1.72	1.64	2.05
64	12.4	2.69	15	2.08	1.65	1.56	1.87
128	9.61	2.09	23	1.87	1.56	1.47	1.69
256	7.55	1.64	39	1.67	1.46	1.37	1.51
512	5.96	1.30	71	1.50	1.37	1.29	1.37
1024	4.72	1.03	135	1.36	1.28	1.20	1.24

^aD and D/2a are explained in the text.

We note that the shape of potential decays for linear and nonlinear approximations differ little for both models. The differences are much more essential between the models. First of all, it is associated with different values of ionic strength at equal surfactant concentrations (forth column of Tables 1 and 2). Values of the relative Debye length $\Lambda = (a + \lambda)/a$, calculated in linear approximation for different surfactant concentrations in both models, are given for subsequent comparison.

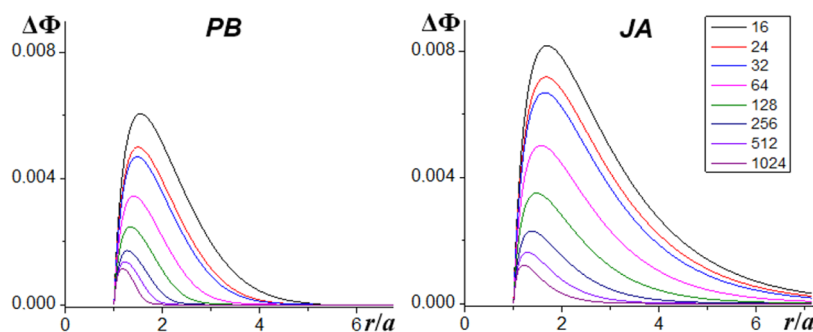


Figure 3. Difference of dimensionless electrostatic potential $\Delta\Phi$ calculated for two close CMC values 8.3 and 8.0 mM as a function of r/a within the PB (left) and JA (right) models in order of increasing surfactant concentration from top to bottom.

The tables also show the distance between centers of micelles D at various concentrations of SDS, calculated by formula

$$D = [N_{\text{agg}}/(C - C_{\text{CMC}})N_A]^{1/3} \quad (8)$$

and the radius of spheres per micelle, $D/2a$, in relative units (N_A is Avogadro's number).

For nonlinear approximation, a slower decrease in potential curves is observed for the JA model. A comparison of numerical data, obtained for dimensionless potential, indicates the right shift of the central part of curves for the PB model and the left shift for the JA model. They correspond to the increase in the effective thickness of the ionic atmosphere for the PB model and its decrease for the JA model for highly charged spherical particles indicating a convergence of results obtained within different models for nonlinear approximation. We also note the nonzero values of potential at the boundaries between micelles, starting from the concentration of $C = 64$ mM, which can lead to the appearance of a self-consistent field and the ordered arrangement of micelles in solution.

RESULTS AND DISCUSSION

Calculation of Micelle Boundaries. For the case of highly charged particles, it is possible to use eq 7, which allows making numerical calculations of dimensionless potential decay at various surfactant concentrations. The shape of potential decay curves allow us to suggest the presence of an uneven decrease in the bulk density of counterions with the increase of the distance from the micellar particle. As is clearly seen in Figure 2 (more clearly demonstrated for high surfactant concentrations), a very fast potential decay turns sharply into a very slow one. Since the enlarged counterion concentration near micelle can be associated with the increased solution viscosity, the breakpoint of these curves can be compared with the hydrodynamic radius of micelles. However, it is difficult to determine this distance only from Figure 2. The situation is aggravated by the fact that the curves were calculated numerically and their analytical function is unknown.

The approach proposed by us, which takes into account small variations in CMC, is free from this drawback. It allows one to determine the position of a surface separating the total diffuse layer from the region with the increased concentration of counterions, which may be a consequence of increased viscosity of solvent surrounding micelle. Therefore, there is every reason to consider this surface as the slipping (shear) surface and to correlate the obtained distance with the micelle hydrodynamic radius.

So, to estimate micelle hydrodynamic radius, the following estimation procedure was carried out. To model the small fluctuations of the micelle microenvironment we solved eq 7 for two close CMC values, namely 8.3 and 8.0 mM. For every of two models a couple of sets ($C_{\text{CMC}} = 8.3$ and 8.0 mM) for dimensionless micelle potential with the same values of main parameters, corresponding to SDS micelles, was calculated. The analysis of difference curves $\Delta\Phi = \Phi_8 - \Phi_{8.3}$ of the dimensionless potentials Φ_8 and $\Phi_{8.3}$, calculated for two CMC values, making it possible to determine the domain of the diffuse layer, in which alterations of the counterion concentration take place. The location of this domain, namely the distance r_{max} corresponding to the maximum amplitude of difference curves, indicates a breakpoint of potential decay, i.e., it can be correlated with the radius of the micelle slipping plane r_ζ (Figure 3).

For both the PB and JA models difference curves have a clearly visible maximum. The analysis of obtained results shows that the calculated positions r_{max}/a of the $\Delta\Phi$ maxima are close to the relative Debye length Λ (see Tables 1 and 2). For the nonlinear approximation, when the use of the Debye length Λ is incorrect, the position r_{max}/a of the $\Delta\Phi$ maxima can be chosen as a parameter related to the micelle hydrodynamic radius. The numerical estimations of such regions of active counterion redistribution, caused by fluctuations in the micellar microenvironment, can be carried out for any arbitrary shape of potential decay.

To find the correlation between parameters Λ and r_{max}/a for linear approximation, the analysis of extremes for difference curves was performed analytically. The functional dependencies Φ_8 and $\Phi_{8.3}$, determined by eq 6 have small discrepancies because of the difference in parameter λ depending on I , and thereby, on the CMC. The resulting difference function $\Delta\Phi = \Phi_8 - \Phi_{8.3}$ was analyzed for extreme as a function of relative distance r/a . For this purpose, we found the r/a values at which the derivative of the difference function reaches zero. It was found that for linear approximation the relative Debye length $\Lambda = (a + \lambda)/a$ and position of the difference function $\Delta\Phi$ maximum, namely the relative distance r_{max}/a , is related to each other by a quadratic equation, which allows us to write the ratio

$$r_{\text{max}}/a = 0.5 + (0.25 + \lambda/a)^{1/2} = 0.5 + (\Lambda - 0.75)^{1/2} \quad (9)$$

The generalization of relation (9) made it possible to calculate parameter Λ in a nonlinear approximation.

Comparison of the Calculated Data with the Experiment. The r_{max}/a concentration dependencies, calculated in

linear and nonlinear approximations, are shown in Figure 4. The lower solid curve corresponds to the PB model and the

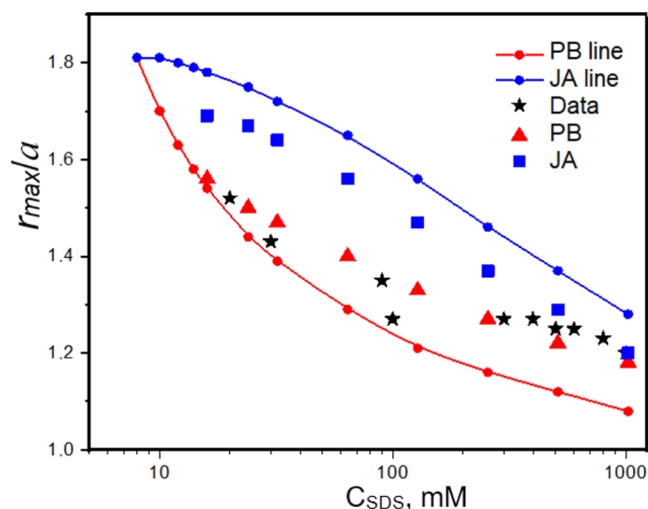


Figure 4. Calculated r_{\max}/a values for linear (solid curves) and nonlinear approximations (triangles - PB model, squares - JA model) and values $(a+T_{\text{shell}})/a$ (asterisks) calculated from the SAXS experiment on hydrophilic layer thickness T_{shell} for SDS micelles.³²

upper one to the JA model. For nonlinear approximation, namely for real micelles, the positions r_{\max}/a are shown by triangles (PB model) and squares (JA model). The analysis of data, presented in Figure 4, indicates that the points corresponding to nonlinear approximation are shifted toward larger distances in comparison with linear case in the PB model and toward shorter distances in the JA model. Similar alterations were observed when we compared the decay of dimensionless potential Φ as a function of relative distance in both cases under consideration. In addition, the values r_{\max}/a for difference curves in both models differ much less for nonlinear approximation than for the linear one. It is important that the results obtained for highly charged particles within both models are in an agreement and their difference does not exceed 10%.

In addition to theoretically calculated values of r_{\max}/a , one can see in Figure 4 the experimental data on the hydrophilic layer thickness for SDS micelles (asterisks), obtained by us previously using small-angle X-ray scattering (SAXS).³² These data, obtained in the form of concentration dependence of micelle hydrophilic layer thickness T_{shell} can be considered as a definite estimation of micelle electric double layer thickness. For comparison, we recalculated our previous experimental data to a relative form $(a + T_{\text{shell}})/a$ for the same radius of the micelle core as was taken before, namely $a = 2.3$ nm. One can see that the results of theoretical calculations are in good agreement with our present experimental data (Figure 4). It is also remarkable that at low surfactant concentrations the experimental values are described more correctly by the PB model, while at concentrations more than 100 mM, when the intermicellar interactions cannot be neglected, the JA model proves to be preferable. However, with concentration increase micelles are distributed more evenly and described better by the JA model.

Estimation of Micelle Boundaries. To clarify the physical–chemical meaning of parameter r_{\max}/a , the values of dimensionless potential $\Phi(r_{\max}/a)$ were estimated. It turns

out that $\Phi(r_{\max}/a)$ values are almost unchanged in the range of studied surfactant concentrations with small discrepancies only at large concentrations. The values of $\Phi(\Lambda)$ did not exhibit this trend. Moreover, our calculations show that in the PB model the micelle electrostatic potential at distance r_{\max} is about 2.5 times less than its maximum value $\Psi(a) = -82$ V at the micelle core surface and about 3 times less for the JA model. For both models $\Psi(a)$ corresponds to -30 mV, i.e., to the threshold of dispersion stability.⁵¹ Moreover, ζ -potential of SDS micelles in the absence of salts turned out to be -27 mV.⁶⁷ On the contrary, the obtained $\Phi(\Lambda)$ values are too small to correspond to the ζ -potential. Both these facts allowed us to suggest that the calculated value of r_{\max} can be taken as the estimate of micelle hydrodynamic radius or shear surface radius r_{ζ} (micelle size) and that the potential on this surface can be compared with the electrokinetic or ζ -potential.

Thus, even in linear approximation for the estimation of the micelle hydrodynamic radius, it is more appropriate to use the r_{\max} value calculated with the help of eq 9. This equation can be extended to the case of highly charged spherical particles. The data presented in Tables 1 and 2 show that the discrepancy between the Debye length for linear and nonlinear variants does not exceed 12%. This means that an approximate estimation of micelle hydrodynamic radius is possible without a numerical solution of differential eq 7. In addition, eq 9 in the form of

$$\begin{aligned} r_{\max}/a &= 0.5 + (0.25 + \lambda/a)^{1/2} \\ &= 0.5 + [0.25 + (\epsilon\epsilon_0 kT/2e^2 I a^2)^{1/2}]^{1/2} \end{aligned} \quad (10)$$

can be applied to find micelle hydrodynamic radius for any surfactant if data on the micelle core radius and the magnitude of ionic strength of solution at a certain temperature are available. It should also be noted that the dependence of sufficiently close values such as $a + \lambda$ and r_{\max} on temperature and ionic strength of solution has a fundamentally different character as follows from eq (10).

The data presented in Tables 1 and 2 allow the determination of micelle characteristic size r_{\max} , which is close to or identical to the micelle hydrodynamic radius in the presence of weak thermal effects. For greater correctness of calculations, one should restrict himself to surfactant concentrations that do not greatly exceed the CMC, since with the increase in concentration, surfactant micelles rather quickly lose their spherical shape and alter the size. At low concentrations, the PB model is preferable. In this case, the r_{\max}/a values are close to 1.5, giving a hydrodynamic radius of about 3.5 nm for SDS micelles. Also, interesting results were obtained when estimating the number of molecular layers of water, located between the micellar particle surface (inner Stern plane) and shear surface with radius r_{\max} (slipping plane). Since the thickness of this layer is approximately $r_{\max} - a = 1.2$ nm it cannot contain more than 5 molecular layers of water with its molecular size of about 0.27–0.3 nm. Of course, in the Stern layer water is strongly ordered and forms the highly packed pseudophase⁶⁸ but the value of 5 layers cannot be greatly exceeded.

The obtained results confirm the hypothesis that the micelle hydrodynamic slipping plane is located near the outer Stern plane and separated from it by only two or three molecular layers of water. The influence of effects, which are stronger than the thermal ones, can shift the slipping plane closer to the micelle core. Therefore, it can be assumed that the smallest

micelle hydrodynamic size is determined by the outer Stern plane, namely, it is limited by the distance at which the quantum-mechanical interactions are manifested, linking surfactant ions and counterions to the solvent-separated ion pairs.

The proposed approach can be extended to study other physicochemical effects in micellar solutions of surfactants. In particular, the suggested approach can be applied to study the influence of external electrolytes or nanoparticles on micellar systems, which will affect the characteristic properties of systems, including the CMC values.^{12,13,69}

CONCLUSIONS

In this work, the existing concepts of the structure of ionic surfactant micelles were refined. By numerically solving the Poisson equation for the two most frequently used approximations, the Poisson–Boltzmann (PB) and the Jellium-approximation (JA) models, the electrostatic potential decay caused by a micelle particle was determined. All calculations were made under the assumption that the composition of a micellar particle of a solid-like dispersed phase in a liquid dispersion medium includes adsorbed counterions rigidly bound to this particle. The shape of decay curves indicates the presence of an uneven decrease in the bulk density of counterions with the increase of distance from the micellar particle. The inflection point of the potential decay curve can be correlated with the position of the micelle hydrodynamic radius. For its determination, the difference curves corresponding to small alterations in the CMC value were considered. Since different experimental techniques give only average CMC values, we assumed that the proposed approach will take into account small fluctuations in the micelle microenvironment, which are inevitable during the micellar transition. Difference curves show that at certain distances from the micelle core there is a region of the counterion density (concentration) redistribution with a well-defined maximum. The position of this maximum is correlated with the boundary separating the region with high solution viscosity and increased concentration of counterions near the micelle from the total diffuse layer in the solution bulk. The obtained distance was recognized as the micelle hydrodynamic radius.

So, we have developed a new methodological approach that allows one to determine the parameter approximately corresponding to the micelle hydrodynamic radius and to calculate the micelle electrokinetic potential. The results of theoretical calculations were compared with our previous experimental data on the thickness of the hydrophilic layer of SDS micelles obtained in SAXS experiments. Good agreement between the calculated and measured data was obtained. It was shown that at low surfactant concentrations, the experimental values are more correctly described by the PB model and at concentrations above 100 mM, when the interactions between micelles cannot be neglected, the JA model is preferable.

The number of molecular layers of water located between the surface of the micellar particle (inner Stern plane) and micelle slipping plane was estimated as not more than five. This confirms the hypothesis that the micelle hydrodynamic slipping plane is located near the outer Stern plane and is separated from it by only a few molecular layers of water. Because of different impacts, stronger than the thermal one, and a shift in the slipping plane closer to the micelle core, it can be assumed that the smallest micelle hydrodynamic size

will be determined by the outer Stern plane. The results of our work allow us to conclude that in fact, a micelle is not something soft and watery, but from its structural properties it is found to be much more a solid-like particle than previously assumed.

Various options for estimating the ionic strength of ionic surfactants micellar solutions, the correlation of calculated and experimental data was discussed. It was noted that the suggested approach can be extended to other effects in surfactant micellar solutions, in particular, to study the influence of external electrolytes or nanoparticles.

AUTHOR INFORMATION

Corresponding Author

Yuriy F. Zuev – Kazan Institute of Biochemistry and Biophysics, FRC Kazan Scientific Center, Russian Academy of Sciences, Kazan 420111, Russia; orcid.org/0000-0002-6715-2530; Email: yufzuev@mail.ru

Authors

Olga S. Zueva – Kazan State Power Engineering University, Kazan 420066, Russia

Vladimir S. Rukhlov – Kazan State Power Engineering University, Kazan 420066, Russia

Complete contact information is available at:

<https://pubs.acs.org/10.1021/acsomega.1c06665>

Notes

The authors declare no competing financial interest.

ACKNOWLEDGMENTS

This work was partly supported by the government assignment for the Federal Research Center Kazan Scientific Center of Russian Academy of Sciences (Y.F.Z.) and by the Federal grant to support the development of academic leadership “Priority 2030” (O.S.Z. and V.S.R.).

REFERENCES

- (1) *Surfactants Science and Technology. Retrospects and Prospects*; Romsted, L. S., Ed.; CRC Press, Taylor & Francis Group: Boca Raton, 2014.
- (2) Rosen, M. J.; Kunjappu, J. T. *Surfactants and Interfacial Phenomena*, 4th ed.; JohnWiley & Sons: New Jersey, 2012.
- (3) *Micelles: Structural Biochemistry, Formation and Functions & Usage*; Bradburn, D.; Bittinger, J., Eds.; Nova Science Publishers: New York, 2013.
- (4) Schramm, L. L.; Stasiuk, E. N.; Marangoni, D. G. Surfactants and their applications. *Annu. Rep. Prog. Chem., Sect. C: Phys. Chem.* **2003**, *99*, 3–48.
- (5) Shaban, S. M.; Kang, J.; Kim, D.-H. Surfactants: Recent advances and their applications. *Compos. Commun.* **2020**, *22*, No. 100537.
- (6) Nowrouzi, I.; Mohammadi, A. H.; Manshad, A. K. Chemical Enhanced Oil Recovery by Different Scenarios of Slug Injection into Carbonate/Sandstone Composite Oil Reservoirs Using an Anionic Surfactant Derived from Rapeseed Oil. *Energy Fuels* **2021**, *35*, 1248–1258.
- (7) Han, X.; Lu, M.; Fan, Y.; Li, Y.; Holmberg, K. Recent Developments on Surfactants for Enhanced Oil Recovery. *Tenside Surf. Det.* **2021**, *58*, 164–176.
- (8) Kesarwani, H.; Saxena, A.; Mandal, A.; Sharma, S. Anionic/Nonionic Surfactant Mixture for Enhanced Oil Recovery through the Investigation of Adsorption, Interfacial, Rheological, and Rock Wetting Characteristics. *Energy Fuels* **2021**, *35*, 3065–3078.

- (9) Malkin, A. Ya.; Zuev, K. V.; Arinina, M. P.; Kulichikhin, V. G. Modifying the Viscosity of Heavy Crude Oil Using Surfactants and Polymer Additives. *Energy Fuels* **2018**, *32*, 11991–11999.
- (10) Singh, R.; Mohanty, K. K. Synergy between Nanoparticles and Surfactants in Stabilizing Foams for Oil Recovery. *Energy Fuels* **2015**, *29*, 467–479.
- (11) Vaisman, L.; Wagner, H. D.; Marom, G. The role of surfactants in dispersion of carbon nanotubes. *Adv. Colloid Interface Sci.* **2006**, *128–130*, 37–46.
- (12) Zueva, O. S.; Makshakova, O. N.; Idiyatullin, B. Z.; Faizullin, D. A.; Benevolenskaya, N. N.; Borovskaya, A. O.; Sharipova, E. A.; Osin, Yu.N.; Salnikov, V. V.; Zuev, YuF. Structure and properties of aqueous dispersions of sodium dodecyl sulfate with carbon nanotubes. *Russ. Chem. Bull.* **2016**, *65*, 1208–1215.
- (13) Zueva, O. S.; Kusova, A. M.; Makarova, A. O.; Turanov, A.; Iskhakova, A.; Salnikov, V. V.; Zuev, Y. F. Reciprocal effects of multi-walled carbon nanotubes and oppositely charged surfactants in bulk water and at interfaces. *Colloids Surf. A: Physicochem. Eng. Asp.* **2020**, *603*, 125296–125304.
- (14) Lombardo, D.; Kiselev, M. A.; Magazù, S.; Calandra, P. Amphiphiles Self-Assembly: Basic Concepts and Future Perspectives of Supramolecular Approaches. *Adv. Condens. Matter Phys.* **2015**, *2015*, 151683–151705.
- (15) Lunardi, C. N.; Gomes, A. J.; Rocha, F. S.; De Tommaso, J.; Patience, G. S. Experimental methods in chemical engineering: Zeta potential. *Can. J. Chem. Eng.* **2021**, *99*, 627–639.
- (16) Duplâtre, G.; Marques, Ferreira; da Gracía, M. F. Miguel, M. Size of Sodium Dodecyl Sulfate Micelles in Aqueous Solutions as Studied by Positron Annihilation Lifetime Spectroscopy. *J. Phys. Chem. A* **1996**, *100*, 16608–16612.
- (17) Bockstahl, F.; Duplâtre, G. Quantitative determination of a sodium dodecyl sulfate micellar radius through positron annihilation lifetime spectroscopy. *Phys. Chem. Chem. Phys.* **1999**, *1*, 2767–2772.
- (18) Bockstahl, F.; Pachoud, E.; Duplâtre, G.; Billard, I. Size of sodium dodecyl sulphate micelles in aqueous NaCl solutions as studied by positron annihilation lifetime spectroscopy. *Chem. Phys.* **2000**, *256*, 307–313.
- (19) Hayter, J. B.; Penfold, J. Determination of micelle structure and charge by neutron small-angle scattering. *Colloid Polym. Sci.* **1983**, *261*, 1022–1030.
- (20) Hartland, G. V.; Grieser, F.; White, L. R. Surface potential measurements in pentanol–sodium dodecyl sulphate micelles. *J. Chem. Soc. Faraday Trans. 1* **1987**, *83*, 591–613.
- (21) Almgren, M.; Swarup, S. Size of sodium dodecyl sulfate micelles in the presence of additives i. alcohols and other polar compounds. *J. Colloid Interface Sci.* **1983**, *91*, 256–266.
- (22) Varela, A. S.; Sánchez, M. I.; Gil, A. The size of sodium dodecyl sulfate micelles in the presence of n-alcohols as determined by fluorescence quenching measurements. *Colloid Polym. Sci.* **1995**, *273*, 876–880.
- (23) Bastiat, G.; Grassl, B.; Khoukh, A.; Francois, J. Study of sodium dodecyl sulfate-poly(propylene oxide) methacrylate mixed micelles. *Langmuir* **2004**, *20*, 5759–5769.
- (24) Molero, M.; Andreu, R.; González, D.; Calvente, J. J.; López-Pérez, G. An isotropic model for micellar systems: application to sodium dodecyl sulfate solutions. *Langmuir* **2001**, *17*, 314–322.
- (25) Ali, A.; Bhushan, V.; Malik, N. A.; Behera, K. Study of Mixed Micellar Aqueous Solutions of Sodium Dodecyl Sulfate and Amino Acids. *Colloid J.* **2013**, *75*, 357–365.
- (26) Mazer, N. A.; Benedek, G. B.; Carey, M. C. An investigation of the micellar phase of sodium dodecyl sulfate in aqueous sodium chloride solutions using quasielastic light scattering spectroscopy. *J. Phys. Chem. B* **1976**, *80*, 1075–1085.
- (27) Corti, M.; Deglorgio, V. Quasielastic Light Scattering Study of Intermicellar Interactions in Aqueous Sodium Dodecyl Sulfate Solutions. *J. Phys. Chem. C* **1981**, *85*, 711–717.
- (28) Colafemmina, G.; Fiorentino, D.; Ceglie, A.; Carretti, E.; Fratini, E.; Dei, L.; Baglioni, P.; Palazzo, G. Structure of SDS Micelles with Propylene Carbonate as Cosolvent: a PGSE-NMR and SAXS Study. *J. Phys. Chem. B* **2007**, *111*, 7184–7193.
- (29) Mirgorod, Y.; Chekadanov, A.; Dolenko, T. Structure of micelles of sodium dodecyl sulfate in water: an X-ray and dynamic light scattering study. *Chem. J. Mold.* **2019**, *14*, 107–119.
- (30) Dunstan, D. E.; White, L. R. An electrokinetic study of micellar solutions. *J. Colloid Interface Sci.* **1990**, *134*, 147–151.
- (31) *Handbook of Microemulsion Science and Technology*; Kumar, P.; Mittal, K. L.; Eds., CRC Press, Taylor & Francis Group: New York, 2018.
- (32) Gubaidullin, A. T.; Litvinov, I. A.; Samigullina, A. I.; Zueva, O. S.; Rukhlov, V. S.; Idiyatullin, B. Z.; Zuev, YuF. Structure and dynamics of concentrated micellar solutions of sodium dodecyl sulfate. *Russ. Chem. Bull.* **2016**, *65*, 158–166.
- (33) Zuev, Yu.F.; Kurbanov, R. Kh.; Idiyatullin, B. Z.; Us'yarov, O. G. Sodium Dodecyl Sulfate Self-Diffusion in Premicellar and Low-Concentrated Micellar Solutions in the Presence of a Background Electrolyte. *Colloid J.* **2007**, *69*, 444–449.
- (34) Moreira, L.; Firoozabadi, A. Molecular Thermodynamic Modeling of Specific Ion Effects on Micellization of Ionic Surfactants. *Langmuir* **2010**, *26*, 15177–15191.
- (35) Zuev, YuF.; Gnezdilov, O. I.; Zueva, O. S.; Us'yarov, O. G. Effective self diffusion coefficients of ions in sodium dodecyl sulfate micellar solutions. *Colloid J.* **2011**, *73*, 59–64.
- (36) Gnezdilov, O. I.; Zuev, YuF.; Zueva, O. S.; Potarikina, K. S.; Us'yarov, O. G. Self-Diffusion of Ionic Surfactants and Counterions in Premicellar and Micellar Solutions of Sodium, Lithium and Cesium Dodecyl Sulfates as Studied by NMR-Diffusometry. *Appl. Magn. Reson.* **2011**, *40*, 91–103.
- (37) Perinelli, D. R.; Cespi, M.; Lorusso, N.; Palmieri, G. F.; Bonacucina, G.; Blasi, P. Surfactant Self-Assembling and Critical Micelle Concentration: One Approach Fits All? *Langmuir* **2020**, *36*, 5745–5753.
- (38) Gillespie, D.A.J.; Hallett, J. E.; O Elujoba, O.; Hamzah, A.F.C.; Richardson, R. M.; Bartlett, P. Counterion condensation on spheres in the salt-free limit. *Soft Matter* **2014**, *10*, 566–577.
- (39) Israelachvili, J. *Intermolecular and Surface Forces*; Academic Press: Amsterdam, 2011.
- (40) *Principles of Colloid and Surface Chemistry, Revised and Expanded*, 3rd ed.; Hiemenz, P. C.; Rajagopalan, R., Eds.; CRC Press: Boca Raton, 1997.
- (41) Rusanov, A. I.; Shchekin, A. K. Mizelloobrazovanie v rastvorakh poverkhnostno-aktivnykh veshchestv. *Micelle Formation in the Solutions of Surfactants*; Lan: St. Peterburg, 2016 (in Russian).
- (42) Stern, O. ZUR Theorie der elektrolytischen Doppelschicht. *Z. Electrochem.* **1924**, *30*, 508–516.
- (43) Rusanov, A. I. The wonderful world of micelles. *Colloid J.* **2014**, *76*, 121–126.
- (44) Grahame, D. C. The Electrical Double Layer and the Theory of Electrocapillarity. *Chem. Rev.* **1947**, *41*, 441–501.
- (45) van der Vegt, N. F. A.; Haldrup, K.; Roke, S.; Zheng, J.; Lund, M.; Bakker, H. J. Water-Mediated Ion Pairing: Occurrence and Relevance. *Chem. Rev.* **2016**, *116*, 7626–7641.
- (46) Farafonov, V. S.; Lebed, A. V.; Mchedlov-Petrosyan, N. O. Character of Localization and Microenvironment of Solvatochromic Reichardt's Betaine Dye in Sodium n-Dodecyl Sulfate and Cetyltrimethylammonium Bromide Micelles: Molecular Dynamics Simulation Study. *Langmuir* **2017**, *33*, 8342–8352.
- (47) Mchedlov-Petrosyan, N. O.; Vodolazkaya, N. A.; Kamneva, N. N. In *Micelles: Structural Biochemistry, Formation and Functions & Usage*; Bradburn, D.; Bittinger, J., Eds.; Nova Publishers: New York, 2013.
- (48) Farafonov, V. S.; Lebed, A. V.; Mchedlov-Petrosyan, N. O. Computing pKa Shifts Using Traditional Molecular Dynamics: Example of Acid–Base Indicator Dyes in Organized Solutions. *J. Chem. Theory Comput.* **2020**, *16*, 5852–5865.
- (49) Bogotsky, V. S. *Fundamentals of Electrochemistry*; Wiley-Interscience: Hoboken, New Jersey, 2006.

- (50) Lyklema, J.; Overbeek, J. Th. G. On the interpretation of electrokinetic potentials. *J. Colloid Sci.* **1961**, *16*, 501–512.
- (51) Greenwood, R.; Kendall, K. Electroacoustic studies of moderately concentrated colloidal suspensions. *J. Eur. Ceram.* **1999**, *19*, 479–488.
- (52) Kralchevsky, P. A.; Danov, K. D.; Broze, G.; Mehreteab, A. Thermodynamics of ionic surfactant adsorption with account for the counterion binding: effect of salts of various valency. *Langmuir* **1999**, *15*, 2351–2365.
- (53) Nakahara, H.; Shibata, O.; Moroi, Y. Examination of Surface Adsorption of Sodium Chloride and Sodium Dodecyl Sulfate by Surface Potential Measurement at the Air/Solution Interface. *Langmuir* **2005**, *21*, 9020.
- (54) Beresford-Smith, B.; Chan, D.Y.C. Electrical double-layer interactions in concentrated colloidal systems. *Faraday Discuss Chem. Soc.* **1983**, *76*, 65–75.
- (55) Beresford-Smith, B.; Chan, D.Y.C.; Mitchell, D. J. The electrostatic interaction in colloidal systems with low added electrolyte. *J. Colloid Interface Sci.* **1985**, *105*, 216–234.
- (56) Danov, K. D.; Kralchevsky, P. A.; Ananthapadmanabhan, K. P. Micelle–monomer equilibria in solutions of ionic surfactants and in ionic–nonionic mixtures: A generalized phase separation model. *Adv. Colloid Interface Sci.* **2014**, *206*, 17–45.
- (57) Danov, K. D.; Basheva, E. S.; Kralchevsky, P. A.; Ananthapadmanabhan, K. P.; Lips, A. The metastable states of foam films containing electrically charged micelles or particles: experiment and quantitative interpretation. *Adv. Colloid Interface Sci.* **2011**, *168*, 50–70.
- (58) Shah, S. S.; Saeed, A.; Sharif, Q. M. A study of micellization parameters and electrostatic interactions in micellar solution of sodium dodecyl sulfate. *Colloids Surf. A: Physicochem. Eng. Asp.* **1999**, *155*, 405–412.
- (59) Joshi, J. V.; Aswal, V. K.; Bahadur, P.; Goyal, P. S. Role of counterion of the surfactant molecule on the micellar structure in aqueous solution. *Curr. Sci.* **2002**, *83*, 47–49.
- (60) Shanks, P. C.; Franses, E. I. Estimation of Micellization Parameters of Aqueous Sodium Dodecyl Sulfate from Conductivity Data. *J. Phys. Chem. D* **1992**, *96*, 1794–1805.
- (61) Ohshima, H. *Electrical Phenomena at Interfaces and Biointerfaces: Fundamentals and Applications in Nano-, Bio-, and Environmental Sciences*; John Wiley & Sons, Inc.: Hoboken, New Jersey, 2012.
- (62) Vautier-Giongo, C.; Bales, B. L. Estimate of ionization degree of ionic micelles based on Krafft temperature measurements. *J. Phys. Chem. B* **2003**, *107*, 5398–5403.
- (63) Bales, B. L. A definition of the degree of ionization of a micelle based on its aggregation number. *J. Phys. Chem. B* **2001**, *105*, 6798–6804.
- (64) Kitzhofer, G.; Koch, O.; Pulverer, G.; Simon, Ch.; Weinmüller, E. *BVPSUITE A New Matlab Solver for Singular/Regular Boundary Value Problems in ODEs*; ACS: Wien, 2010.
- (65) López-García, J.; Moya, A. A.; Horno, J.; Delgado, A.; Gonzalez-Caballero, F. A. Network Model of the Electrical Double Layer around a Colloid Particle. *J. Colloid Interface Sci.* **1996**, *183*, 124–130.
- (66) Loeb, A. L.; Overbeek, J. ThG.; Wiersema, P. H. *The Electrical Double Layer Around a Spherical Colloid Particle*; MIT Press: Cambridge, MA, 1961.
- (67) Brown, W.; Zhao, J. Adsorption of sodium dodecyl sulfate on polystyrene latex particles using dynamic light scattering and zeta potential measurements. *Macromolecules* **1993**, *26*, 2711–2715.
- (68) Mirgorod, YuA.; Dolenko, T. A. Liquid Polyamorphous Transition and Self-Organization in Aqueous Solutions of Ionic Surfactants. *Langmuir* **2015**, *31*, 8535–8548.
- (69) Zueva, O. S.; Rukhlov, V. S.; Gazeeva, E. V.; Mongush, Y. K. Mathematical modeling of surfactant self-organization in water solution in the presence of carbon nanotubes. *IOP Conf. Ser. Earth Environ. Sci.* **2019**, *288*, 012059–012066.